

Siponimod (BAF312) penetrates, distributes, and acts in the central nervous system: Preclinical insights

Marc Bigaud , Bettina Rudolph, Emmanuelle Briard, Christian Beerli, Andreas Hofmann , Erwin Hermes, Florian Muellershausen, Anna Schubart and Anne Gardin

Multiple Sclerosis Journal—
Experimental, Translational
and Clinical

October-December 2021,
1–13

DOI: 10.1177/
20552173211049168

© The Author(s), 2021.
Article reuse guidelines:
sagepub.com/journals-
permissions

Abstract

Background: Siponimod (BAF312), a selective S1P₁/S1P₅ agonist, reduces disability progression in secondary progressive MS. Recent observations suggest it could act via S1P₁/S1P₅-dependent anti-inflammatory and pro-myelination effects on CNS-resident cells.

Objective: Generate preclinical evidence confirming siponimod's CNS penetration and activity.

Methods: Siponimod's CNS penetration and distribution was explored in rodents and non-human primates (NHPs) using: Liquid Chromatography coupled to tandem Mass Spectrometry (LC-MS/MS), quantitative whole-body autoradiography (QWBA) using ¹⁴C-radiolabeled siponimod or non-invasive single-photon emission CT (SPECT) with a validated ¹²³I-radiolabeled siponimod analog. Functional CNS activity was investigated by S1P₁ receptor quantification in brain homogenates.

Results: In mice/rats, siponimod treatments achieved dose-dependent efficacy and dose-proportional increase in drug blood levels, with mean brain/blood drug-exposure ratio (_{Brain/Blood}DER) of 6–7. Efficacy in rat brain tissues was revealed by a dose-dependent reduction in brain S1P₁ levels. QWBA distribution analysis in rats indicated that [¹⁴C]siponimod related radioactivity could readily penetrate CNS, with particularly high uptakes in white matter of cerebellum, corpus callosum, and medulla oblongata versus lower exposures in other areas such as olfactory bulb. SPECT monitoring in NHPs revealed CNS distribution with a _{brain/blood}DER of ~6, as in rodents.

Conclusion: Findings demonstrate siponimod's CNS penetration and distribution across species, with high translational potential to human.

Keywords: Siponimod, CNS penetration, rodents, non-human primates, quantitative whole-body autoradiography, and single-photon emission computed tomography

Date received: 20 April 2021; revised: 24 August 2021; accepted 27 August 2021

Introduction

Siponimod is the first oral disease-modifying therapy shown to reduce disability progression, cognitive decline, total brain volume loss, gray matter atrophy, and signs of demyelination in secondary progressive multiple sclerosis (SPMS) patients.^{1–3} It is a potent and selective agonist for two of the five known membrane G-protein-coupled receptors for sphingosine-1-phosphate (S1P)-receptor subtypes 1 and 5 (S1P₁ and S1P₅) that has demonstrated robust immunomodulatory, anti-inflammatory, pro-myelination, and

neuroprotective properties in various preclinical models.^{4–7} It was recently approved, as Mayzent®, for the treatment of relapsing forms of MS, including clinically isolated syndrome, relapsing-remitting disease (RRMS), and SPMS, in adults (USA)⁸ and for SPMS patients with active disease (Europe).⁹

The immunomodulatory properties of siponimod involve S1P₁-dependent retention of blood-pathogenic lymphocytes within secondary lymphoid organs, as established previously for fingolimod

Correspondence to:
Marc Bigaud,
Novartis Institutes for
BioMedical Research
(NIBR), Novartis Pharma
AG, Forum 1, Novartis
Campus CH-4056 Basel,
Switzerland.
marc.bigaud@novartis.com

Marc Bigaud,
Novartis Institutes for
BioMedical Research, Basel,
Switzerland



Bettina Rudolph,
Novartis Institutes for
BioMedical Research, Basel,
Switzerland

Emmanuelle Briard,
Novartis Institutes for
BioMedical Research, Basel,
Switzerland

Christian Beerli,
Novartis Institutes for
BioMedical Research, Basel,
Switzerland

Andreas Hofmann,
Novartis Institutes for
BioMedical Research, Basel,
Switzerland

Erwin Hermes,
Novartis Institutes for
BioMedical Research, Basel,
Switzerland

Florian Muellershausen,
Novartis Institutes for
BioMedical Research, Basel,
Switzerland

Florian Muellershausen,
Novartis Institutes for
BioMedical Research, Basel,
Switzerland

Florian Muellershausen,
Novartis Institutes for
BioMedical Research, Basel,
Switzerland

Florian Muellershausen,
Novartis Institutes for
BioMedical Research, Basel,
Switzerland

Florian Muellershausen,
Novartis Institutes for
BioMedical Research, Basel,
Switzerland

Anna Schubart,
Novartis Institutes for
BioMedical Research, Basel,
Switzerland

Anne Gardin,
Novartis Institutes for
BioMedical Research, Basel,
Switzerland

(FTY720, Gilenya®), the prototype S1P-modulator approved as an oral agent for RRMS,^{10,11} and for all the S1P₁ agonists described thus far.^{12,13} The underlying molecular mechanisms involve internalization and degradation (down-modulation or functional antagonism) of S1P₁ receptors on pro-inflammatory T- and B-lymphocytes.¹⁰ Consequently, lymphocytes become unresponsive to the S1P gradient, depriving them of an obligatory signal to egress from secondary lymphoid organs and thus preventing their recirculation to susceptible target organs such as the central nervous system (CNS).

In addition, siponimod's apparent anti-inflammatory, pro-myelination, and neuroprotective properties might be attributable to S1P₁/S1P₅-dependent effects on CNS-resident cells, as strongly suggested by numerous preclinical observations.^{4,6,14–16} Understanding siponimod's mechanism of action therefore requires exploration of its ability to penetrate and distribute within CNS tissues. A first set of evidence supporting CNS penetration for siponimod was obtained in mice¹⁷; and the present study aimed to consolidate these observations by assessing CNS penetration/distribution for siponimod, and siponimod-related radioactive material (siponimod and/or metabolites), in rodents and in a more translational relevant preclinical species such as non-human primates (NHPs).^{18,19}

Materials and methods

Animals and animal welfare

All studies in rodents were performed in accordance with protocols approved by the Cantonal Veterinary Office of Basel and according to regulations defined by the European Community Council Directive for animal protection. Briefly, adult female C57BL/6J mice (18–19 g; Charles River or Harlan Laboratories Switzerland) and male Long Evans or Han:Wistar rats (220–230 g; Janvier, France/Harlan, The Netherlands) were group housed and had free access to tap water and standard diet (Maus/Ratte Haltung GLP, KLIBA NAFAG-3890; Provimi Kliba AG, Switzerland). Housing rooms were temperature controlled (22 ± 2°C) throughout the study period. Animal housing, care, and experimental use were conducted according to the Swiss Federal Law for animal protection.

Studies in NHPs were carried out under institutional animal care protocols complying with US-Federal regulations. Animal housing/care approval and oversight was provided by the Rush University, Chicago, Illinois IACUC. Briefly, 2 male rhesus macaques

(*Macaca mulatta*) housed at the Rush University Medical Center in Chicago (Illinois, USA) were used for SPECT imaging. Imaging was conducted under institutional animal care protocols complying with Federal regulations.

Experimental protocols

Studies in mice. These studies aimed at measuring siponimod concentrations in blood and brain in mice treated with siponimod-loaded diet for at least 10 days at various doses. Mice were either healthy or subject to experimental autoimmune encephalomyelitis (EAE):

- **In healthy mice:** C57BL/6 mice were randomized in treatment groups (n = 6/group) and fed for 10 days with siponimod-loaded food pellets (prepared as described in Supplementary Information) at various doses, 0.1, 0.3, 1, 10, and 30 mg siponimod/kg of food, to achieve drug uptakes of about 0.3, 1, 3, 30, and 100 µg/day, respectively (when considering a mean daily food uptake of ~3 g/day). At termination, mice were deeply anesthetized with oxygen/isoflurane (97/3, v/v; isoflurane: Forene®, Abbott AG, Switzerland). Terminal blood samples (~100 µL) and brain tissues were collected for measuring the blood lymphocyte counts and the siponimod levels via LC-MS/MS. As all terminations were performed early mornings (~2 h after start of day light), the measured drug levels correspond to the peak drug exposures, considering that mice eat about 70–80% of their food during the night.
- **In EAE mice:** Female C57BL/6 mice (12 weeks old) were randomized so all groups had similar mean body weights (n = 6–10/group). Siponimod treatment started on day-0 by introducing siponimod-loaded food pellets at 0, 3, 10, 30, 100 or 200 mg siponimod/kg of food (corresponding to drug uptakes of about 0, 10, 30, 100, 300 and 600 µg/day, respectively). On the same day (day-0), EAE was induced as described in the Supplementary information.

Studies in rats. These studies aimed at, 1 – Measuring siponimod concentrations in blood, plasma, brain and CSF at various time points after repeated oral dosing; 2-Assessing siponimod-induced down-modulation of S1P₁ receptors in brain after repeated oral dosing; 3-Performing quantitative whole-body autoradiography (QWBA) at various time points after repeated oral dosing of [¹⁴C]siponimod hemifumarate.

- Rat studies with non-radiolabeled siponimod:
 - *Rat study 1:* Long Evans rats were treated daily by oral gavage over 7 days with siponimod at 0.01, 0.1, and 1 mg/kg/day ($n = 3$ /group). At 8 h after the last treatment, terminal blood and CSF samplings were performed under deep anesthesia with oxygen/isoflurane mixture (Forene®). Bodies were then perfused for 8 min, via a left ventricle cannula, with ice-cold phosphate-buffered saline before collecting the whole brain. Hemispheres were separated, weighed and placed onto dry ice before storage at -80°C until further use, one side for siponimod content via LC-MS/MS, the other side for the level of S1P₁ receptors.
 - *Rat study 2:* Han:Wistar rats were treated daily by oral gavage over 7 days with siponimod at 3 mg/kg. On the last treatment day, terminal blood ($\sim 200\ \mu\text{L}$), CSF ($\sim 20\ \mu\text{L}$) and brain samplings were performed, under deep Forene® anesthesia, at 8, 24, 72, or 168 h post-last dosing ($n = 2-3$ /time point). Plasma samples were prepared by centrifugation (2000 g) of blood aliquots at 4°C for 10 min. All blood, plasma, CSF and brain samples were stored at -80°C until further processing for siponimod content via LC-MS/MS.
- Rat studies with radiolabeled siponimod:
 - Male Long Evans rats were treated daily by oral gavage over 7 days with [¹⁴C]siponimod hemifumarate at 3 mg/kg (dose referring to base). On the last treatment day, rats were terminated via deep Forene® anesthesia at 8, 24, 72, or 168 h post-dose ($n = 1$ /time point) and blood samples ($\sim 200\ \mu\text{L}$) collected via sublingual vein puncturing for radioactivity determination by liquid scintillation counting (LSC). The carcasses were processed for QWBA analysis (details in Supplementary Information) to assess the distribution of [¹⁴C]siponimod related radioactivity over time to the various CNS regions.

Studies in NHPs. These studies aimed at monitoring, in 2 male rhesus macaques, siponimod brain penetration and distribution, via non-invasive single-photon emission CT (SPECT), using a specific tracer (MS565), a previously validated ¹²³I-radiolabeled imaging analog for siponimod.¹⁷ Parts of these works were previously reported.²⁰ Details concerning the SPECT analysis are described in Supplementary Information.

Treatment materials

All test materials used in different studies were supplied by Novartis, Basel, Switzerland (see Supplementary Information).

Analysis of biological samples

The whole blood lymphocyte counts were measured with the use of an ADVIA 120 Hematology System with MultiSpecies Software [BAYER].

Plasma samples were prepared by centrifugation (2000 g for rodent, 3000g for NHP) of blood aliquots at 4°C for 10 min. All blood, plasma, and brain tissue samples were stored at -80°C until further processing for siponimod content via LC-MS/MS or radioactivity measurements. Further technical details concerning analysis of biological samples collected are described in the Supplementary Information.

Data analysis

For the EAE study, clinical score comparisons between treatment groups were evaluated on a daily basis and compared to vehicle control. All statistical analyses of clinical score parameters used a Mann-Whitney rank sum test For S1P₁ levels in tissues, a parametric Student's T-test was utilized. All statistical analyses were performed using GraphPad Prism version 6 for Windows, (GraphPad Software, USA). Statistical significance was set at $p < 0.05$.

Results

Siponimod penetrates mouse CNS in a dose-proportional manner and protects against the development of EAE

Both healthy and EAE mice fed with siponimod-loaded food pellets showed dose-proportional steady-state siponimod levels in blood and brain homogenates, with markedly higher levels in brains for all siponimod doses tested (Figure 1). Similar siponimod levels were determined in the cerebral cortex versus rest of brain, although there was a trend for the levels to always be the lowest in the cortex.

In healthy mice, the dose-proportional increase in siponimod blood levels resulted in a dose-dependent reduction in blood lymphocyte counts (Figure 2(a)), with a maximal reduction of about 80% achieved at a diet-loading dose of 10 mg/kg (approximately equivalent to a daily drug intake of 30 μg /mouse or 1.5 mg/kg). At this dose, the mean siponimod levels achieved in whole blood and brain homogenates were within the 500 nM and 3 μM ranges, respectively. Higher drug exposures did not induce stronger reduction in blood lymphocytes. For all doses tested, the mean drug-exposure ratio between brain homogenates and blood ($_{\text{Brain/Blood}}\text{DER}$) approached 6,

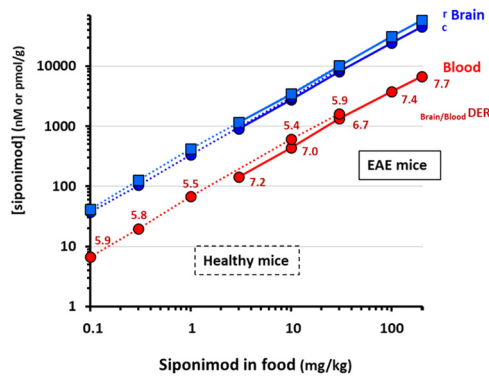


Figure 1. Dose-proportional steady-state siponimod levels in healthy and EAE mice. Healthy and EAE mice were fed for several days with siponimod-loaded food pellets at various concentrations (0.1 to 200 mg of siponimod per kg of food). Steady-state siponimod concentrations reached in blood and brain homogenates are shown (c, cortex; r, rest of the brain). Dotted lines link results obtained in healthy mice whereas plain lines are used for EAE mice. Blood concentrations are expressed as nM and in brain as pmol/g (equivalent to nM). All points are mean \pm SEM (n = 6–10). For each dose tested, the mean $\text{Brain/Blood}^{\text{DER}}$ was calculated.

suggesting a steady CNS penetration for siponimod across a wide dose-range.

In EAE mice, the dose-proportionality of the siponimod levels in blood and brain homogenates were aligned with those seen in healthy mice. As blood drug levels tended however to be a bit lower than in healthy mice, a mean $\text{Brain/Blood}^{\text{DER}}$ around 7 was found for all doses tested (Figure 1). In addition, all the siponimod doses tested were efficacious at significantly reducing the blood lymphocyte counts by 70–80% ($p < 0.05$; details not shown), as well as the development of EAE scores ($p < 0.05$), with a

maximal efficacy obtained at the diet-loading dose of 10 mg/kg (Figure 2(b)). At this dose, the mean siponimod levels in whole blood and brain homogenates were within the 400–500 nM and 3–3.5 μM ranges, respectively. Higher drug exposures did not result in significantly stronger protection against EAE.

Siponimod penetrates rat CNS and is pharmacologically active

The siponimod concentrations in blood, plasma, brain homogenates, and CSF measured 8 h post-last treatment in rats treated for 7 consecutive days with siponimod at 0.01, 0.1, or 1 mg/kg/day (rat study 1) are shown in Figure 3(a). Siponimod concentrations in blood and plasma were within the same range and increased in a dose dependent manner, reaching the 2-, 12-, and 120-nM range at 0.01, 0.1, and 1 mg/kg/day, respectively. Nearly 6-fold higher drug levels were measured in brain homogenates (i.e. ~16, 70 and 700 nM range, respectively), indicating $\text{brain/blood}^{\text{(DER)}}$ or $\text{brain/plasma}^{\text{(DER)}}$ around 6, as in mice. In CSF, siponimod concentrations within 0.2 nM were detected only with the highest treatment dose of 1 mg/kg/day, indicating a CSF/brain ratio reaching 0.0003 and therefore suggesting that the siponimod measured in brain tissues was mostly (>99.9%) bound to tissues.

The siponimod concentrations achieved in brains were associated with a dose-dependent down-modulation of S1P₁ receptors in brain homogenates, as indicated by measurements of S1P₁ protein levels (Figure 3(b)). There was no significant effect for siponimod at 0.01 mg/kg/day (~16 nM in brain tissues) and average reductions of 36% and 78% in S1P₁ protein levels were observed for siponimod at 0.1

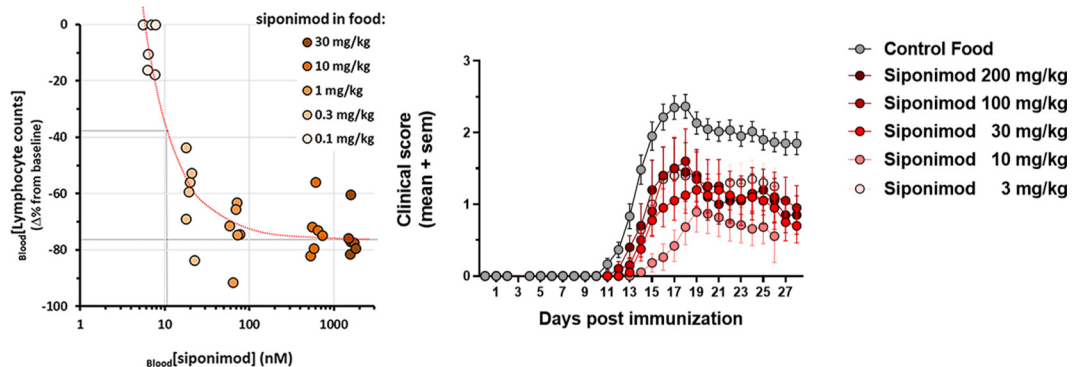


Figure 2. (a) individual blood lymphocyte counts measured in naive mice fed over 10 days with diet loaded with siponimod at 0.1, 0.3, 1, 10 and 30 mg/kg. (b) Longitudinal changes in mean EAE severity scores in mice fed with a siponimod-loaded diet at 3, 10, 30, 100 or 200 mg/kg of food (n = 6–10/treatment group). SEM, standard error of the mean.

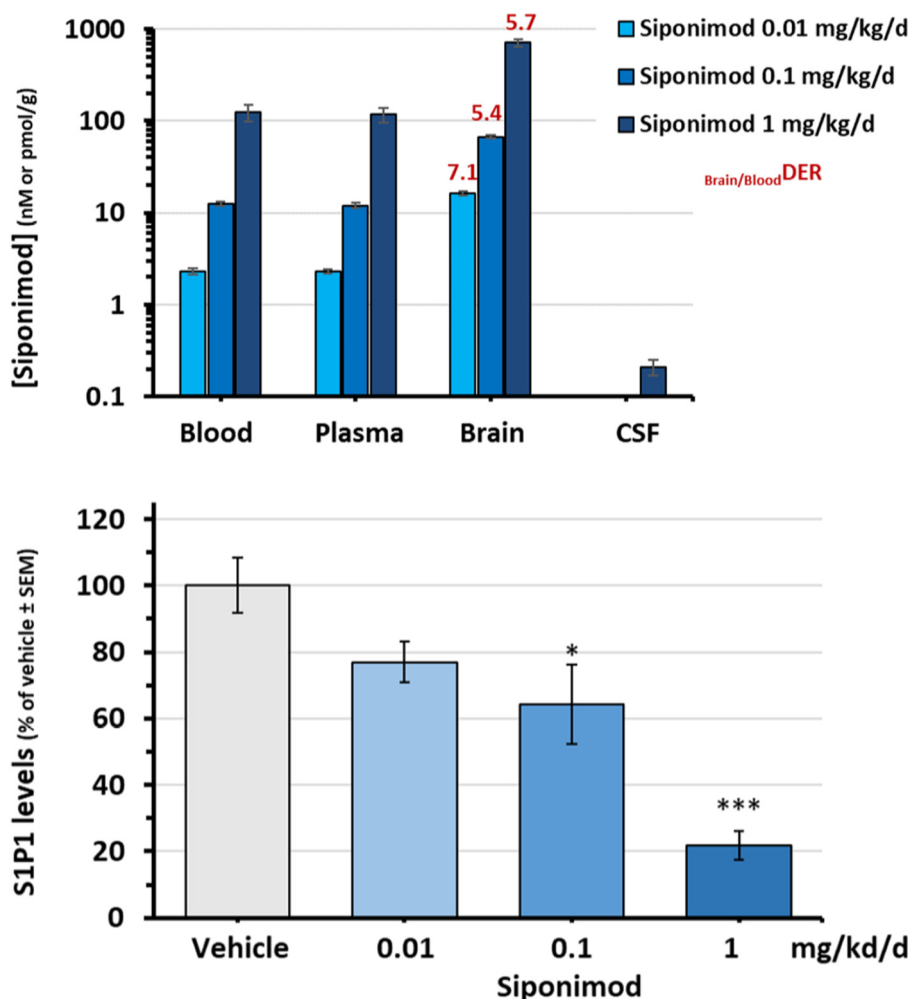


Figure 3. Dose-dependent siponimod levels in rats. Rats were treated orally for 7 days with siponimod at 0.01, 0.1, and 1 mg/kg/day ($n = 3/\text{group}$): (a) Siponimod concentrations in blood, plasma, brain, and CSF, at 8 h after the last treatment. Blood, plasma, and CSF concentrations are expressed in nM and brain levels in pmol/g (equivalent to nM); (b) Mean amount of S1P₁ protein detected in the brain homogenates of the treated rats, as expressed in % versus vehicle-treated group. * $p < 0.05$, *** $p < 0.005$. CSF, cerebrospinal fluid; DER, drug-exposure ratio; S1P, sphingosine 1-phosphate; SEM, standard error of the mean.

and 1 mg/kg/day (~70 and 700 nM in brain tissues), respectively, versus vehicle control.

To track siponimod concentrations over time in plasma versus brain and CSF, rats were treated with 3 mg/kg/day siponimod and samples were collected at 8, 24, 72, and 168 h after the last treatment (rat study 2). The plasma siponimod levels measured at 8 h post-treatment reached a mean concentration range of 0.7 μM , whereas ~3-fold higher levels were measured in brain (2.3 μM) (Table 1). Simultaneously, mean siponimod concentrations within the 6 nM range were detected in CSF, *i.e.* 340-fold lower compared to brain. At 24 h post-last treatment, siponimod concentrations in plasma, brain, and CSF were reduced

versus 8 h values by 90%, 50%, and 70%, respectively. At 72 h post-treatment, siponimod could no longer be detected in plasma and CSF but was still measurable in brains (~35 nM range).

Taken together, these results suggest siponimod's dose-proportional CNS penetration and efficacy on S1P₁ receptors in rats, with specific kinetic profiles in plasma, brain tissues and CSF. The markedly lower concentrations of siponimod measured in CSF versus brain tissues suggest that siponimod measured in CNS tissues is mostly (>99.9%) bound to tissues. This is in line with previous studies proposing that drug levels measured in the CSF are surrogate measurements for brain unbound concentrations.²¹

Table 1. Concentrations of siponimod in plasma, brain, and CSF following 7 daily oral doses at 3 mg/kg/day to Han:wistar rats. Measurements were performed in samples collected at different time points (8, 24, 72, and 168 h) after the last treatment.

Time point (h)	Mean [range] concentrations			Brain/ Plasma ^{DER}
	Plasma (μM)	Brain (nmol/g)	CSF (μM)	
8 (n = 2)	0.688 [0.548–0.838]	2.30 [2.26–2.34]	0.00666 [0.00288–0.01043]	3.3
24 (n = 2)	0.0711 [0.029–0.114]	1.16 [0.741–1.572]	0.00195 [0–0.00389]	16.3
72 (n = 3)	<LOQ	0.0351 [0.0302–0.0366]	<LOQ	–
168 (n = 3)	<LOQ	<LOQ	<LOQ	–

Limit of quantification (LOQ) for plasma: 0.0019 nM. A similar value was considered for brain and CSF. Values below LOQ were set to 0.
CSF: cerebrospinal fluid; DER: drug-exposure ratio.

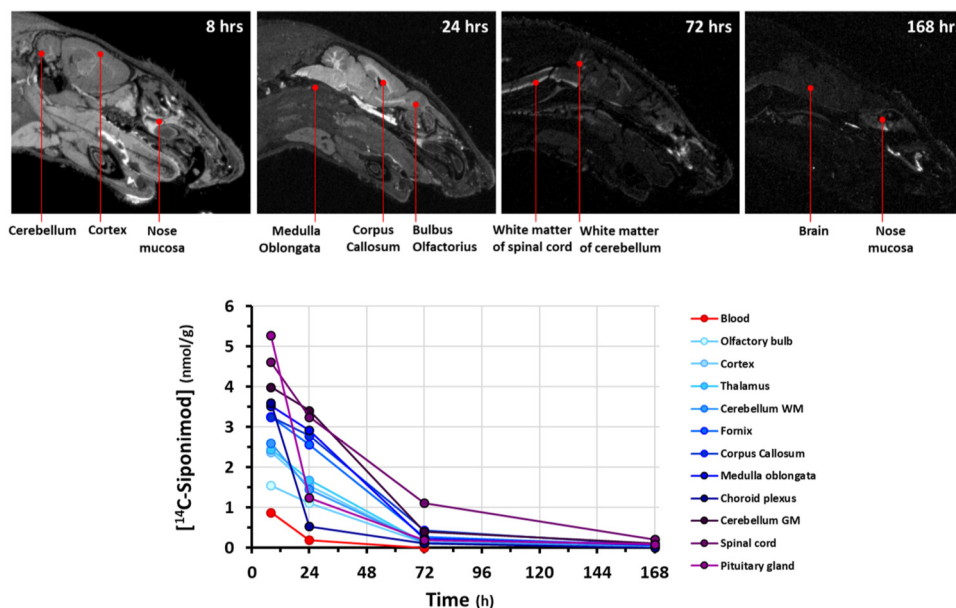


Figure 4. QWBA analysis after repeated oral dosing with [^{14}C]siponimod. Male Long Evans rats were treated orally for 7 days with [^{14}C]siponimod hemifumarate at a dose of 3 mg/kg/day (dose referring to base; n = 1/time point): (a) Quantitative whole-body autoradiograms, focusing on the head region, collected at 8, 24, 72, and 168 h after the last oral dose are shown. The carcasses were cut longitudinally through the middle. The whitest area corresponds to the highest radioactivity concentration; (b) Tissue concentration over time courses of total radiolabeled components in blood and different brain regions. GM, gray matter; QWBA, Quantitative Whole Body Autoradiography; WM, white matter.

[^{14}C]siponimod-related radioactivity distributes throughout CNS in rats

Rats were treated orally for 7 days with [^{14}C]siponimod hemifumarate at 3 mg/kg/day (dose referring to base), and the amount of radioactivity (reflecting siponimod and/or its metabolites) was determined using QWBA at 8, 24, 72, and 168 h after the last treatment. Representative examples of whole-body autoradiographs focusing on the head region are shown in

Figure 4(a). Concentration time courses of [^{14}C] siponimod-related radioactivity measured in various brain regions are shown in Figure 4(b). The corresponding calculated tissue PK parameters are listed in Table 2.

Following 7 daily oral doses of 3 mg/kg/day [^{14}C] siponimod hemifumarate, the related radioactivity was taken up into the brain extensively with areas

Table 2. Pharmacokinetic parameters of total radiolabeled components after multiple oral doses of 3 mg/kg/day [¹⁴C]siponimod hemifumarate (dose referring to base) in long evans rats.

Tissues	T _{max} (h)	C _{max} (nmol/g)	C _{max} ^a ratio	AUC _{last} (h*nmol/g)	AUC _{last} ^a ratio	T _{last} (h)	T _{1/2} (h)	Range for T _{1/2} (h)
Blood (QWBA)	8	0.917	1.00	12.6	1.00	24	NC	NA
Blood (LSC)	8	0.881	0.960	12.1	0.960	24	NC	NA
Brain (cerebellum, gray matter)	8	2.60	2.83	89.2	7.08	168	NC	NA
Brain (cerebellum, white matter)	8	3.99	4.35	191	15.1	168	NC	NA
Brain (cerebral cortex)	8	2.38	2.60	88.8	7.05	168	NC	NA
Brain (choroid plexus)	8	3.60	3.93	62.9	5.00	72	NC	NA
Brain (corpus callosum)	8	3.25	3.54	163	12.9	168	28.6	24–168
Brain (fornix)	8	3.26	3.55	143	11.3	168	28.0	24–168
Brain (inferior colliculus)	8	2.90	3.16	107	8.46	168	NC	NA
Brain (medulla oblongata)	8	3.52	3.84	156	12.4	168	NC	NA
Brain (olfactory bulb)	8	1.55	1.69	65.1	5.17	168	NC	NA
Brain (superior colliculus)	8	2.95	3.21	106	8.42	168	NC	NA
Brain (thalamus)	8	2.44	2.66	95.8	7.60	168	NC	NA
Spinal cord	8	4.61	5.02	249	19.8	168	36.8	24–168
Spinal cord (gray matter)	8	3.40	3.70	124	9.84	168	NC	NA
Spinal cord (white matter)	8	4.37	4.77	292	23.2	168	50.1	24–168

^aNormalized to blood value (i.e. Tissue/blood ratio).
AUC_{last}: Area under the concentration-time curve from time zero to time of last measurable concentration; C_{max}: maximum plasma concentration; LSC: liquid scintillation counting; NA: not applicable; NC: not calculated due to the limited data set; QWBA: quantitative whole-body autoradiography; T_{max}: time taken to reach C_{max}; T_{last}: time of last measurable concentration; T_{1/2}: elimination half-life.

under the concentration-time curves from time zero to the last measurable concentration normalized to blood AUC_{last} (AUC_{last} tissue/blood ratios) of 5.0–23.2, suggesting regional differences for the distribution of [¹⁴C]siponimod-related radioactivity in the CNS. Highest AUC_{last} tissue/blood ratios were observed for spinal cord (white matter (23.2), the white matter of cerebellum (15.1), corpus callosum (12.9), and medulla oblongata (12.4). Interestingly, about 2-fold higher siponimod exposures could be observed in white versus gray matters of the brain and spinal cord (Table 2).

Siponimod penetrates CNS in NHPs

Two rhesus macaques received a single intravenous bolus injection of [¹²³I]MS565 and were monitored over 3 days for brain SPECT imaging. A representative example of the [¹²³I]MS565 SPECT monitoring is shown in Figure 5(a). Overall, [¹²³I]MS565 displayed good brain penetration, with brain-tissue uptake (particularly marked in cortical and thalamic areas) increasing over 26–32 h post-injection and then slowly washing out up to 48 h. Quantitative analysis of these SPECT images resulted in a more precise kinetic of drug uptake (expressed as standard

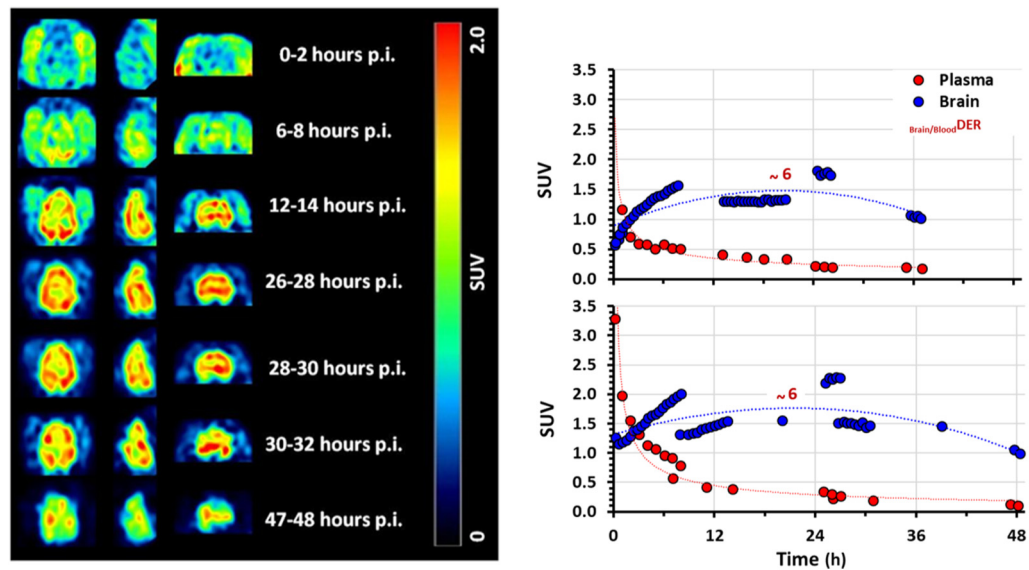


Figure 5. SPECT-imaging of the siponimod analog ($[^{123}\text{I}]\text{MS565}$) in rhesus NHPs. In rhesus macaques ($n=2$) that received one single intravenous bolus injection of ^{123}I -radiolabeled analog of siponimod ($[^{123}\text{I}]\text{MS565}$): (a) Representative examples of $[^{123}\text{I}]\text{MS565}$ SPECT brain images over time (transverse, left; sagittal, middle; coronal, right). Increase in brain uptake is visible within 26–30 h post-injection, followed by a slow washout; (b) Decay-corrected time-activity curves (expressed as standard uptake value (SUV)) for the mean $[^{123}\text{I}]\text{MS565}$ concentrations in both blood and brain tissues measured in both NHPs tested (RH8355 and RH8356). In both cases, washout of $[^{123}\text{I}]\text{MS565}$ from the plasma started immediately upon injection and was nearly completed (>90%) within 24 h. In contrast, peak brain uptake occurred within 18–24 h post-injection, with a $\text{Brain}/\text{Blood DER}$ of about 6 and followed by a slow decay. GM, gray matter; h, hour; MRI, magnetic resonance imaging; NHP, non-human primate; SPECT, Single Photon Emission Computed Tomography; SUV, standard uptake value.

uptake value (SUV) by brain tissues) (Figure 5(b)) and revealed a peak CNS uptake within 18–24 h post-injection. At that time, the $[^{123}\text{I}]\text{MS565}$ levels measured in plasma suggest that its elimination from plasma was nearly completed (>90%) and indicate a $\text{Brain}/\text{Plasma DER}$ of ~ 6 , as seen in mice and rats.

To better analyze the distribution of $[^{123}\text{I}]\text{MS565}$ within the different brain regions, SPECT and T1-weighted MRI images obtained over 7–48 h post-injection were merged (Figure 6(a)). This analysis suggested that a small fraction of $[^{123}\text{I}]\text{MS565}$ reached the brain ventricles and that different uptake might exist between white and gray matter. The comparative dynamic uptake of $[^{123}\text{I}]\text{MS565}$ for cortical gray matter and white matter is shown in Figure 6(b), together with a polynomial fit to the data from both animals. Hence, drug uptake (expressed as SUV) increased up to 18–20 h post-injection to reach up to ~ 1.6 in gray matter versus 1.8 in white matter (0.011% vs 0.012% injected dose (ID)/mL, respectively), suggesting a 13% preference uptake for white matter. Washout of $[^{123}\text{I}]\text{MS565}$ appeared faster in gray versus white matter, with SUV at 48 h post-injection reduced to ~ 0.9 in

gray matter and ~ 1.25 in white matter (0.006% vs 0.008% ID/mL, respectively), suggesting a 39% preference residual uptake for white matter.

Discussion

The aim of the present investigations was to generate preclinical insights concerning the CNS penetration, distribution, and activity of siponimod, thus, elucidating its direct pharmacological effects in the CNS to help explain its therapeutic benefit in SPMS.³

The first compelling evidence on the central efficacy for SIP_1 agonists, in addition to their inhibitory effects on lymphocyte trafficking, came from a study showing that fingolimod had lost therapeutic efficacy in an EAE model using conditional null mouse mutants lacking SIP_1 receptors on astrocytes but not on lymphocytes.²² Since then, observations accumulated supporting SIP_1 -dependent effects in the CNS for fingolimod,²³ as well as siponimod.^{4,6,14–16} The molecular events downstream of the SIP_1 receptors remain to be fully understood as both SIP_1 down-modulation and activation of signaling pathways involved in the regulation of astrocyte survival and proliferation have been described.^{16,24,25} Recently, siponimod was shown to induce, in human

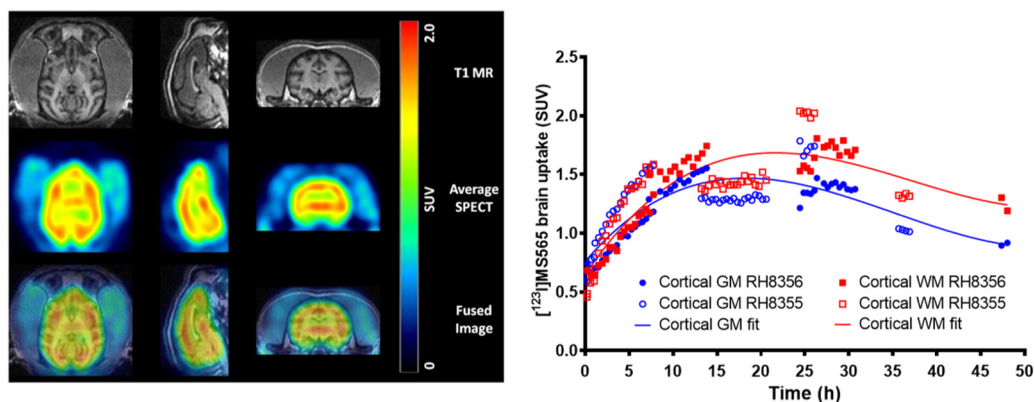


Figure 6. Uptake of [^{123}I]MS565, an imaging siponimod analog in different brain regions. Rhesus macaques received a single intravenous bolus injection of [^{123}I]MS565: (a) Representative example of an average SPECT image of NHP brain over 7–48 h post-injection fused with a T1-weighted MRI (MRI [top], [^{123}I]MS565 SPECT brain average image [middle] and fused MRI-SPECT image [bottom]). Transverse images are left, sagittal images are middle, and coronal images are right; (b) Decay-corrected time–activity curves displaying an increase in the activity concentration of [^{123}I]MS565 in the brain until ~ 20 h after injection, followed by a faster washout in the gray matter (GM) versus white matter (WM). The solid line represents a polynomial fit. Closed symbols for NHP-RH8356 and open symbols for NHP-RH8355. GM, gray matter; MRI, magnetic resonance imaging; NHP, non-human primate; SUV, standard uptake value; WM, white matter.

astroglial cells, an S1P₁-dependent activation of the anti-oxidant/ anti-inflammatory/neuroprotective transcription factor Nrf2 in parallel to the blockade of the pro-inflammatory transcription factor NF κ B.²⁶ Less is known about central S1P₅-dependent effects on oligodendrocytes, although they were shown to be mainly pro-myelinating.^{6,15}

Concerning CNS penetration of siponimod, previous preclinical studies in mice suggested that it could be achieved upon a single intravenous bolus application with, at ≤ 8 h post-dosing, a maximal blood exposure associated with a markedly higher (~ 5 fold) drug levels in brain tissues.¹⁷ The present study confirms these observations in healthy mice, rats and NHPs, strongly suggesting that the ability of siponimod to dose-dependently penetrate and distribute into the CNS compartment is preserved across species, with a Brain/BloodDER maintained within the range of 5–6, independently of the dose or regimen used.

In the mouse, siponimod treatments were applied via drug-loaded diet, as preliminary work indicated that it was a robust alternative to daily oral gavage for achieving efficacious siponimod blood exposures in chronic mouse disease models.²⁷ The present results clearly confirm that such a treatment can indeed achieve a dose-proportional increase in steady state siponimod blood levels and a dose-dependent pharmacological efficacy (reduction in circulating lymphocytes) with a maximal effect at a food-loading dose of 10 mg/kg. As expected, the same food-loading dose of 10 mg/kg

was also found maximally efficacious in reducing the development EAE symptoms, further illustrating the relevance of EAE models as mechanistic tools for studying the anti-inflammatory/immunomodulatory effects of S1P modulators.^{10–13} Interestingly, for all siponimod doses tested in EAE mice, a Brain/BloodDER around 7 was measured, suggesting that the CNS penetration of siponimod is not subject to major changes during the development of the disease.

In the rat, a dose-proportional increase in siponimod blood levels could also be achieved via daily oral gavage with, as in mice, a brain/blood(DER) around 6 for all dose tested. Pharmacological efficacy in the CNS could be demonstrated by a dose-dependent reduction in S1P₁ levels in brain tissues, in line with previous observations describing drug-induced S1P₁ down-modulation in CNS-resident cells^{24,25,28} or brain tissues.^{29,30} For technical reasons, no benchmarking with other S1P receptors could be performed and follow up studies are therefore warranted. Available data however suggest that the S1P₃, S1P₄ and S1P₅ receptors contrast vs S1P₁ upon activation by fingolimod, with partial down-modulation for S1P₃²⁹ and no down-modulation at all for S1P₄^{29,31} and S1P₅.³² Such behaviors of S1P receptors in brain tissues are most likely not affected by the development of central inflammation, as suggested by studies showing that, although the S1P₁ and S1P₃ expressions are increased on astrocytes in MS and EAE lesions, they can be reduced by the administration of fingolimod.^{33,34} Confirmation would certainly

be justified with the help of dedicated EAE studies. Concerning the distribution of siponimod throughout the rat CNS, it was assessed via QWBA analysis which revealed a specific tissue distribution pattern of [^{14}C] siponimod related radioactivity within the different CNS areas, with highest concentration of siponimod related radioactivity detected for the white matter of the cerebellum, corpus callosum, medulla oblongata and spinal cord, and twice as low levels in the olfactory bulb. These results, suggesting that the distribution of siponimod throughout the CNS is subject to marked regional selectivity, motivated follow up confirmatory studies in NHPs.

The clinical relevance of NHPs as a model to predict brain penetration and distribution of drugs in human has been well documented^{18,19} and SPECT imaging in NHPs was previously validated as a translational method to estimate brain penetration of fingolimod.^{35,36} Validation was performed using BZM055, a radiolabeled surrogate for fingolimod that demonstrated similar brain distribution patterns between NHPs and humans. The same approach was therefore followed for evaluating the brain penetration of siponimod in NHPs with [^{123}I]MS565, previously validated as a reliable SPECT tracer for siponimod.^{17,20} SPECT results obtained in the present study indicate good brain penetration for siponimod in NHPs, with high levels versus other tissues surrounding the brain and with particularly high uptake in cortical and thalamic areas, a slight preference for white versus gray matter, and a quite residual appearance in CSF.

Taken together the present investigations demonstrate consistent brain penetration/ distribution for siponimod across species, which is suggestive of a high translational potential to human. Although this type of information is key to confirm that siponimod has the intrinsic properties to physically access CNS-resident cells expressing S1P₁/S1P₅ receptors, it is of semi-qualitative nature and, as such, does not by itself ascertain that local unbound siponimod levels would also reach the concentration range required for biological activity in humans. Additional quantitative imaging studies in humans, with evaluation of receptor occupancy would be an additional helpful next step to provide further evidence to that end.

Available pharmacological data, uncorrected for protein binding, indicate a potency for siponimod on S1P₁/S1P₅ receptors within the 1 nM range⁵ and efficacy on cultured astrocytes or oligodendrocytes

within the 10–100 nM range.^{14–16} Corrected values for the binding-to-brain tissues, as estimated for siponimod in the present study (>99.9%) and fully in line with >99.9% binding-to-plasma protein in human,³⁷ might project that unbound siponimod CNS levels within the 0.01–0.1 nM range could be needed for preclinical in vivo efficacy. Such a range was most likely reached in rats treated with siponimod at 3 and 1 mg/kg/day, as indicated by the drug levels measured in the CSF (~6 and 0.2 nM, respectively), which can be considered as surrogate measurements for brain unbound drug concentrations.²¹ Translation to humans is currently unclear as limited siponimod CSF information in human is at present available and would require dedicated studies using clinical imaging technologies. Of the 1651 patients enrolled in the EXPAND trial,³ only nine (~0.5%) accepted CSF sampling at end of treatment, five of whom could be confirmed as siponimod treated due to occurrence of siponimod (low nM range) in the CSF.

An intriguing observation from the present studies is that the Brain/BloodDER and Brain/PlasmaDER for siponimod were found to be ~6 across the doses and species tested, suggesting persistence along evolution of the underlying mechanisms controlling siponimod's CNS penetration. Despite several investigations, no active transporter for siponimod has been identified as yet (unpublished in house observation), suggesting that its CNS penetration is driven by its high lipophilicity ($\log D_{7.4} = 2.6$)¹⁷ and passive membrane diffusion. In this case, the CNS penetration of siponimod is not expected to be markedly affected by the development of local inflammatory conditions, as supported by a Brain/BloodDER of ~7 found in EAE mice. Although the consistency of Brain/BloodDER and Brain/PlasmaDER across doses and species for siponimod suggests a good translation to human, dedicated studies in healthy volunteers vs MS patients, using clinical imaging technologies, would be warranted to provide confirmation. Benchmarking to other S1P modulators would also clarify pharmacokinetic/pharmacodynamic relationships for different molecules from the same pharmacological class and the possible link between CNS penetration and central efficacy. Hence, available comparative data suggest that, although the CNS penetration for both fingolimod and its active phosphorylated metabolite are similar to siponimod in healthy rodents (with Brain/BloodDER ~6), they increase by at least 3 fold during EAE development,^{38,39} in strong contrast to siponimod. For ozanimod, its CNS penetration is about twice as high vs siponimod and fingolimod in healthy rodents (CNS/BloodDER of

10–16) and the impact of EAE has not been described as yet.⁴⁰ Too high CNS levels might however be counterproductive for S1P modulators to achieve efficacy in the CNS compartment concomitantly to the periphery as recent observations suggest that S1P receptor-dependent central anti-inflammatory, neuroprotective, and/or pro-myelination effects are subject to a non-classical pharmacology, characterized by a loss of efficacy at supramaximal exposures (bell-shaped dose-response curves).^{41–44}

Overall, these preclinical studies suggest a robust dose-proportional CNS penetration/distribution with central pharmacological efficacy for siponimod, with a high translational potential to human. The proportion between specific and unspecific binding to the CNS tissues remains to be established, as well as the pharmacokinetic profile of siponimod in the CNS versus blood. Follow-up preclinical and clinical studies will be helpful to identify the molecular mechanisms controlling siponimod CNS exposure and to fully understand how siponimod distributes within the CNS, in relation to its well-described pharmacodynamic effects (anti-inflammatory, neuroprotective, pro-myelination)^{6,14–16} at the level of CNS-resident cells.

Acknowledgements

All authors met the International Committee of Medical Journal Editors (ICMJE) criteria for authorship for this manuscript, take responsibility for the integrity of the work as a whole, and have given final approval to the version to be published. All authors are responsible for intellectual content and data accuracy. We are grateful to Esther van de Kerkhof, Adriana Tavaréz, Paul Maguire, Olivier Barret, Meike Lang, Lea Baumgartner, Pamela Ramseier, Sarah Tisserand, and Julien Perdoux for their expert technical support. We thank Swetha Sanugomula (Novartis Healthcare, Hyderabad, India) for providing medical writing support, which encompassed formatting of the manuscript content, referencing, tables and figures as per the journal guidelines, and incorporating the authors' revisions and finalizing the draft for submission, all under the direction of the authors.



Declaration of conflicting interests

All authors are employees of Novartis and author(s) declared no potential conflicts of interest with respect to the research, authorship, and/or publication of this article

Funding

Novartis Pharma AG, Basel, Switzerland funded the study and medical writing support for the preparation of this manuscript.

ORCID iDs

Marc Bigaud  <https://orcid.org/0000-0002-1168-5311>
 Andreas Hofmann  <https://orcid.org/0000-0001-5450-6267>

Supplemental material

Supplemental material for this article is available online.

References

1. Arnold DL, Bar-Or A, Cree BAC, et al. Impact of siponimod on myelination as assessed by MTR across SPMS subgroups: post hoc analysis from the EXPAND MRI substudy. *Mult Scler J* 2020; 26: 397–659.
2. Fox R, Arnold D, Giovannoni G, et al. Siponimod reduces grey matter atrophy in patients with secondary progressive multiple sclerosis: subgroup analyses from the EXPAND study (1130). *Neurology*. 2020; 94: 1130.
3. Kappos L, Bar-Or A, Cree BAC, et al. Siponimod versus placebo in secondary progressive multiple sclerosis (EXPAND): a double-blind, randomised, phase 3 study. *Lancet*. 2018; 391: 1263–1273.
4. Behrangi N, Fischbach F and Kipp M. Mechanism of siponimod: anti-inflammatory and neuroprotective mode of action. *Cells*. 2019; 8: 24.
5. Gergely P, Nuesslein-Hildesheim B, Guerini D, et al. The selective sphingosine 1-phosphate receptor modulator BAF312 redirects lymphocyte distribution and has species-specific effects on heart rate. *Br J Pharmacol*. 2012; 167: 1035–1047.
6. Mannioui A, Vauzanges Q, Fini JB, et al. The *Xenopus* tadpole: an in vivo model to screen drugs favoring remyelination. *Mult Scler*. 2018; 24: 1421–1432.
7. Pan S, Gray NS, Gao W, et al. Discovery of BAF312 (siponimod), a potent and selective S1P receptor modulator. *ACS Med Chem Lett*. 2013; 4: 333–337.
8. Mayzent® US Prescribing Information 2019. East Hanover, NJ: Novartis Pharmaceuticals Corporation.
9. Mayzent® summary of product characteristic 2020. Novartis Pharma AG.
10. Brinkmann V, Cyster JG and Hla T. FTY720: sphingosine 1-phosphate receptor-1 in the control of lymphocyte egress and endothelial barrier function. *Am J Transplant*. 2004; 4: 1019–1025.
11. Zecri FJ. From natural product to the first oral treatment for multiple sclerosis: the discovery of FTY720 (gilenya)? *Curr Opin Chem Biol*. 2016; 32: 60–66.
12. Huwiler A and Zangemeister-Wittke U. The sphingosine 1-phosphate receptor modulator fingolimod as a therapeutic agent: recent findings and new perspectives. *Pharmacol Ther*. 2018; 185: 34–49.
13. Juif PE, Krachenbuehl S and Dingemans J. Clinical pharmacology, efficacy, and safety aspects of sphingosine-1-phosphate receptor modulators. *Expert Opin Drug Metab Toxicol*. 2016; 12: 879–895.

14. Cui QL, Fang J, Almazan G, et al. Sphingosine 1-phosphate receptor agonists promote axonal ensheathment by human fetal oligodendrocyte progenitors. *Multi Scler J*. 2011; 17: S366 [P823].
15. Jackson SJ, Giovannoni G and Baker D. Fingolimod modulates microglial activation to augment markers of remyelination. *J Neuroinflammation*. 2011; 8: 76.
16. O'Sullivan C, Schubart A, Mir AK, et al. The dual S1PR1/S1PR5 drug BAF312 (siponimod) attenuates demyelination in organotypic slice cultures. *J Neuroinflammation*. 2016; 13: 31.
17. Briard E, Rudolph B, Desrayaud S, et al. MS565: a SPECT tracer for evaluating the brain penetration of BAF312 (siponimod). *ChemMedChem*. 2015; 10: 1008–1018.
18. Di L, Rong H and Feng B. Demystifying brain penetration in central nervous system drug discovery. Miniperspective. *J Med Chem*. 2013; 56: 2–12.
19. Feng B, Doran AC, Di L, et al. Prediction of human brain penetration of P-glycoprotein and breast cancer resistance protein substrates using In vitro transporter studies and animal models. *J Pharm Sci*. 2018; 107: 2225–2235.
20. Tavares A, Barret O, Alagille D, et al. Brain distribution of MS565, an imaging analogue of siponimod (BAF312), in non-human primates (P1.168). *Neurology*. 2014; 82: P1.168. https://n.neurology.org/content/82/10_Supplement/P1.168.short
21. Liu X, Smith BJ, Chen C, et al. Evaluation of cerebrospinal fluid concentration and plasma free concentration as a surrogate measurement for brain free concentration. *Drug Metab Dispos*. 2006; 34: 1443–1447.
22. Choi JW, Gardella SE, Herra DR, et al. FTY720 (fingolimod) efficacy in an animal model of multiple sclerosis requires astrocyte sphingosine 1-phosphate receptor 1 (S1P1) modulation. *Proc Natl Acad Sci*. 2011; 108: 751–756.
23. Hunter SF, Bowen JD and Reder AT. The direct effects of fingolimod in the central nervous system: implications for relapsing multiple sclerosis. *CNS Drugs*. 2016; 30: 135–147.
24. Mullershausen F, Craveiro LM, Shin Y, et al. Phosphorylated FTY720 promotes astrocyte migration through sphingosine-1-phosphate receptors. *J Neurochem*. 2007; 102: 1151–61.
25. Healy LM, Sheridan GK, Pritchard AJ, et al. Pathway specific modulation of S1P1 receptor signalling in rat and human astrocytes. *Brit J Pharmacol*. 2013; 169: 1114–1129.
26. Colombo E, Bassani C, Angelis AD, et al. Siponimod (BAF312) activates Nrf2 while hampering NFκB in human astrocytes, and protects from astrocyte-induced neurodegeneration. *Frontiers Immunol*. 2020; 11: 635.
27. Dietrich M, Hecker C, Beerli C, et al. Optimising siponimod (BAF312) oral administration for long-term experimental studies in mice. *ECTRIMS On Line Library* 2018; 229455: ePoster EP1618. https://onlinelibrary.ectrims-congress.eu/ectrims/2018/ectrims-2018/229455/philipp.albrecht.optimising.siponimod.28baf31229.oral.administration.for.html?f=menu=6*ce_id=1428*ot_id=20024*media=3*browseby=8
28. Ben Yacoub N, Uffelmann T, Tisserand S, et al. Mouse astrocytes exhibit agonist-induced functional S1P1 receptor antagonism. *ECTRIMS On Line Library* 2020; Poster P0357. https://library.msvirtual2020.org/virtual-library-search?product_id=7
29. Kim S, Bielawski J, Yang H, et al. Functional antagonism of sphingosine-1-phosphate receptor 1 prevents cuprizone-induced demyelination. *Glia*. 2018; 66: 654–669.
30. Brinkmann V, Streiff M, Bigaud M, et al. Fingolimod treatment is associated with a down-modulation of S1P1 receptor protein in the CNS. *Neurology*. 2012; 78(Suppl 1): P02.107. https://n.neurology.org/content/78/1_Supplement/P02.107.short
31. Gräler MH and Goetzl EJ. The immunosuppressant FTY720 down-regulates sphingosine 1-phosphate G protein-coupled receptor. *FASEB J*. 2004; 18: 551-3.
32. Bigaud M, Tisserand S, Fuchs-Loesle P, et al. The S1P5 receptor is not down-modulated in response to selective agonists. *Mult Scler*. 2018; 24(S2): 913 (EP021617).
33. Van Doorn R, Van Horssen J, Verzijl D, et al. Sphingosine 1-phosphate receptor 1 and 3 are upregulated in multiple sclerosis lesions. *Glia*. 2010; 58: 1465–1476.
34. Colombo E, Di Dario M, Capitolo E, et al. Fingolimod may support neuroprotection via blockade of astrocyte nitric oxide. *Ann Neurol*. 2014; 76: 325–337.
35. Briard E, Orain D, Beerli C, et al. BZM055, An iodinated radiotracer candidate for PET and SPECT imaging of myelin and FTY720 brain distribution. *ChemMedChem*. 2011; 6: 667–677.
36. Tamagnan G, Tavares A, Barret O, et al. Brain distribution of BZM055, an analog of fingolimod (FTY720), in human. *Mult Scler J*. 2012; 18: 379.
37. Gardin A, Dodman A, Kalluri S, et al. Pharmacokinetics, safety, and tolerability of siponimod (BAF312) in subjects with severe renal impairment: a single-dose, open-label, parallel-group study. *Int J Clin Pharmacol Ther*. 2017; 55: 54–65.
38. Foster CA, Howard LM, Schweitzer A, et al. Brain penetration of the oral immunomodulatory drug FTY720 and its phosphorylation in the central nervous system during experimental autoimmune encephalomyelitis: consequences for mode of action in multiple sclerosis. *J Pharmacol Exp Ther*. 2007; 323: 469–475.
39. Bigaud M, Tisserand S, Ramseier P, et al. Differentiated pharmacokinetic/pharmacodynamic (PK/PD) profiles for siponimod vs fingolimod. *ECTRIMS On Line Library* 2019; 278982: Poster P622. <https://onlinelibrary.ectrimscongress.eu/ectrims/2019/stockholm/278982/marc.bigaud.differentiated.pharmacokinetic.pharmacodynamic.%28pk.pd%29.profiles.html>
40. Scott FL, Clemons B, Brooks J, et al. Ozanimod (RPC1063) is a potent sphingosine-1-phosphate receptor-1 (S1P1) and receptor-5 (S1P5) agonist with

- autoimmune disease-modifying activity. *Br J Pharmacol*. 2016; 173: 1778–1792.
41. Bigaud M, Tisserand S, Albrecht P, et al. Siponimod: from understanding mode of action to differentiation versus fingolimod (1536). *Neurology*. 2020; 94: 1536.
42. Bigaud MDF, Hach T, Piani Meier D, et al. Dual mode of action of siponimod in secondary progressive multiple sclerosis: a hypothesis based on the relevance of pharmacological properties. *Mult Scler J* 2020; 26: 272–659.
43. Cuzzocrea S, Doyle T, Campolo M, et al. Sphingosine 1-phosphate receptor subtype 1 as a therapeutic target for brain trauma. *J Neurotrauma*. 2018; 35: 1452–1466.
44. Miron VE, Ludwin SK, Darlington PJ, et al. Fingolimod (FTY720) enhances remyelination following demyelination of organotypic cerebellar slices. *Am J Pathol*. 2010; 176: 2682–2694.